



## Mechanistic insights into temperature-responsive deep eutectic solvent for alginate recovery and solvent recycling

Isa S.A. Hiemstra <sup>a</sup>, Faridah Husna <sup>a</sup>, Michel H.M. Eppink <sup>b</sup>, Rene H. Wijffels <sup>a,c</sup>,  
Antoinette Kazbar <sup>a,\*</sup>

<sup>a</sup> Bioprocess Engineering, Wageningen University & Research, PO Box 16 Wageningen, 6700, AA, Wageningen, the Netherlands

<sup>b</sup> TU Delft, Faculty of Applied Sciences, Department of Biotechnology, Van der Maasweg 9, 2629, HZ, Delft, the Netherlands

<sup>c</sup> Nord University, Faculty of Biosciences and Aquaculture, N8049, Bodø, Norway

### ARTICLE INFO

Editor name: M Freire

**Keywords:**

Temperature-responsive deep eutectic solvents  
Solvent recycling  
Brown seaweed  
COSMO-RS  
Sustainable solvent design

### ABSTRACT

Conventional alginate extraction from brown seaweed typically relies on harsh, non-recyclable chemicals, limiting process sustainability. This study presents temperature-responsive deep eutectic solvents (TRDES) as circular, recyclable extractants for alginate recovery. Using computational screening with COSMO-RS and experimental validation of TRDES affinity and alginate partitioning, TRDES1 (o-cresol: ethanolamine) was identified as the most promising combination, and was optimised and reused over eight cycles, yielding up to  $55.6 \pm 14.4$  mg/g DW. COSMO-RS modelling validated the observed increase in extraction efficiency over successive cycles, showing enhanced partition coefficients and reduced Gibbs free energy of transfer with reuse. The process enabled mild extraction of functional alginate with increasing efficiency over the cycles. The main solvent parameters for TRDES design found to govern extraction and recyclability were capacity (C), partition coefficient (K), and Gibbs free energy ( $\Delta G$ ). Optimal performance was achieved with moderate TRDES–water capacity ( $1.27 \times 10^1$  to  $3.15 \times 10^1$ ), low TRDES capacity ( $<1.2$ ), and  $K > 1$ . This work establishes a theoretical framework with design rules for future TRDES development based on computational and experimental analysis and highlights the need for novel, biocompatible TRDES systems. As demonstrated, combining computational screening with these design principles enables the use of recyclable solvents. Incorporating natural compounds into TRDES design enhances both process efficiency and sustainability, facilitating the integration of DES technologies into circular biorefineries and supporting environmentally responsible biomass valorisation.

### 1. Introduction

The valorisation of renewable biomass has become a valuable asset in the development of sustainable and circular bioeconomies. Brown seaweeds are an interesting renewable biomass that can be used for valorisation. These macroalgae contain valuable bioactive compounds, including polysaccharides, proteins, lipids and polyphenols, with antibacterial, antiviral and antifungal properties [1–3]. Among these compounds, alginate is a polysaccharide that is widely used in the food, pharmaceutical, and biomedical industries due to its gel-forming and biocompatible properties [4]. This polysaccharide has a simple molecular structure, containing two uronic acid units, D-mannuronic acid (M)

and L-guluronic acid (G). These two uronic acids are present in varying sequences and ratios and are linked by  $\beta$ -1,4-glycosidic bonds [5] (Fig. S1).

Efficient extraction of these compounds is essential for applications in pharmaceuticals, food, and materials science. However, conventional alginate extraction relies on multiple processing stages that use harsh chemicals, under both acidic and alkaline conditions, resulting in significant water consumption and a high energy input [6]. Moreover, the solvents used in alkaline extraction are typically not recyclable, leading to environmental and economic concerns.

Deep eutectic solvents (DES) have emerged as a promising class of alternative extraction solvents [7]. Formed by the complexation of one

**Abbreviation:** DES, Deep eutectic solvent; TRDES, Temperature-responsive deep eutectic solvent; COSMO-RS, CONductor-like screening MOdel for real solvents; UCST, Upper-critical solution temperature; LCST, Lower critical solution temperature; M/G, Mannuronic to guluronic acid ratio; K, Partition coefficient;  $\gamma$ , Activity coefficient; C, Solvent capacity; FTIR, Fourier-transform infrared spectroscopy; SEC, Size-exclusion chromatography; HBA, Hydrogen bond acceptor; HBD, Hydrogen bond donor; MEA, Monoethanolamine; DEA, Diethanolamine; TEA, Triethanolamine.

\* Corresponding author.

<https://doi.org/10.1016/j.seppur.2026.136807>

Received 27 October 2025; Received in revised form 16 December 2025; Accepted 5 January 2026

Available online 6 January 2026

1383-5866/© 2026 The Author(s). Published by Elsevier B.V. This is an open access article under the CC BY license (<http://creativecommons.org/licenses/by/4.0/>).

or more hydrogen bond donors (HBD) and acceptors (HBA), the depression in melting point leads to the formation of a DES. DES can be classified as green solvents due to their low volatility, high thermal stability, tuneable physicochemical properties, simple preparation without chemical reactions, and the possibility of selecting biocompatible, biodegradable components that can be recycled [8,9], making them attractive candidates as extraction solvents.

DES show significant potential in the extraction of various bioactive compounds from different biomasses. DES have been successfully applied for the extraction of bioactives from various biomasses, including plants [10,11], microalgae [12,13] and seaweed [14,15].

Although alginate was successfully extracted using DES in our previous study, achieving a higher extraction yield compared to conventional processing [16], the main challenge associated with DES is the efficient isolation of the extracted compounds from the solvent and the subsequent recycling of the DES. DES recycling is complicated due to the low vapour pressure DES exhibits [17].

Several approaches have been proposed for DES recovery, including membrane separation [18], antisolvent addition [10,19] and the use of macroporous resins [14]. Nonetheless, these methods often involve additional solvents, a high energy input, or lead to incomplete solvent recovery. Additionally, these studies do not address DES recycling but only focus on extractant recovery. Therefore, efficient recycling strategies are essential to ensure that DES-based processes are not only effective but also reusable and circular.

To address this issue, research has recently turned toward the development of a novel class of DES, known as responsive deep eutectic solvents (RDES) [20]. RDES are a novel subclass of DES designed to undergo physical or chemical changes in response to external stimuli. These systems can respond to external triggers, including carbon dioxide (CO<sub>2</sub>), changes in pH, or temperature, allowing for controlled phase transitions through changes in polarity or solubility that facilitate selective extraction and solvent recovery [20,21]. Among these, temperature-responsive DES (TRDESs) are particularly appealing due to the simplicity of temperature manipulation. By exploiting the reversible solubility in response to temperature shifts, TRDES offer a promising alternative for DES recovery and recycling without the need for additional reagents or complex equipment [21]. TRDES can exhibit either upper (UCST) or lower critical solution temperature (LCST) behaviour. UCST-type systems are immiscible with water at low temperatures due to strong hydrogen bonding between DES components, but become miscible upon heating as thermal energy disrupts these interactions [21,22]. In contrast, LCST behaviour involves phase separation at high temperatures, driven by entropy and the weakening of hydrogen bonds between the DES and water [23].

Despite growing interest in TRDESs, their application in marine biomass extraction remains limited, and fundamental thermodynamic governing extraction, separation, and recyclability are often overlooked. Understanding DES–water–compound affinity and partitioning behaviour is essential for rationally optimising extraction efficiency, phase switching, and solvent recovery. Integrating predictive modelling could offer valuable thermodynamic insights and support the systematic design of DES-based biorefinery processes, rather than relying solely on empirical solvent screening. Such an approach also holds broader potential, enabling the prediction of solvent behaviour across diverse compounds and feedstocks, and guiding the development of more versatile and ultimately more sustainable extraction systems.

Therefore, this study aimed to evaluate the feasibility of extracting and recovering alginate using UCST-type TRDES, with the aim of establishing a mechanistic understanding of TRDES behaviour during extraction and recycling, thereby enabling simultaneous alginate isolation and solvent recovery. First, 22 TRDES were selected and evaluated for their phase switching behaviour. By addressing the solubility capacity and partition coefficient in COSMO-RS (COnductor-like Screening MOdel for Real Solvents), a model used to predict thermodynamic properties of fluids and solutions, the performance of different

TRDES and the alginate partition behaviour was modelled. Subsequently, alginate extraction and recovery were conducted. The optimal TRDES was used, extraction was optimised, and the alginate was characterised. The TRDES fraction could be recycled for up to eight rounds of alginate extraction.

This study provides an effective framework and design criteria that can be translated to the future development of greener and biocompatible TRDES systems. By combining experimental extraction with COSMO-RS modelling, the main solvent parameters for TRDES design that govern extraction and recovery were established. This work contributes to the advancement of deep eutectic solvent (DES) recycling and promotes circularity in extraction processes, supporting the rational design of sustainable and resource-efficient biorefinery approaches.

## 2. Materials & methods

### 2.1. Materials

Brown seaweed *Saccharina latissima* was obtained from Algaia, France, in September 2024. The biomass was freeze-dried, ground, sieved and stored in the dark at 4 °C. Monoethanolamine (>98 %), diethanolamine (>98 %), triethanolamine (>99 %), 2-(Methylamino) ethanol (>98 %), (Dimethylamino)ethanol (>99.5 %), o-cresol (99 %), p-cresol (99 %), m-cresol (99 %), guaiacol, 3-Methoxyphenol (96 %), 4-Methoxyphenol (99 %), L-menthol (99 %), methyltrioctylammonium chloride, decanoic acid (>98 %), phenyl salicylate (99 %), octanoic acid (>98 %) and D-galacturonic acid monohydrate (>97 %), sodium tetraborate (99 %), sulfuric acid (95–98 %), carbazole (>95 %) and ethanol (>99 %) were purchased from Sigma-Aldrich.

### 2.2. TRDES preparation

In total, 22 TRDES were selected for the screening. The TRDESs were prepared by mixing the HBA and HBD at 60 °C until a clear and homogeneous liquid formed. The details of the TRDES formulation tested are listed in Table 1 and Fig. S2.

### 2.3. TRDES screening

#### 2.3.1. Laboratory

The TRDES were first tested to assess whether phase separation would occur between the DES and aqueous phase. Phase separation was examined at 50 % v/v TRDES concentration. The solution was heated to 60 °C in a water bath for one hour and vortexed every 10 min. Then, the solution was refrigerated at 4 °C to allow it to cool down and separate into two phases. If phase separation did not occur in the solution, sodium chloride was added to achieve 8 % salt concentration to facilitate phase separation further [24]. The TRDES that phase separated from the aqueous fraction were then used for alginate extraction, whereas the formulations that did not phase separate were discarded for alginate extraction.

#### 2.3.2. COSMO-RS

2.3.2.1. *TRDES comparison.* The COSMO-RS (Conductor-like Screening Model for Real Solvents) software is an effective computational tool for predicting the thermodynamic behaviour of fluid mixtures [26]. Analyses were performed using COSMO-RS version 2022.103 (Software for Chemistry and Materials BV, Amsterdam, The Netherlands) integrated within the Amsterdam Density Functional (ADF) package. Molecular geometries of all compounds were pre-optimised using the universal force field (UFF), followed by density functional theory (DFT) calculations at the GGA:BP86 level with a TZP basis set [27].

The direct application of COSMO-RS to polymers such as alginate is impractical, as it requires extensive quantum chemical COSMO

**Table 1**

Details of the TRDES used in this study.

	HBAs	HBDs	Molar ratios	Reference
TRDES1	Monoethanolamine	o-cresol	1:1	[22]
TRDES2	Monoethanolamine	p-cresol	1:1	
TRDES 3	Monoethanolamine	m-cresol	1:1	
TRDES 4	Diethanolamine	o-cresol	1:1	
TRDES 5	Diethanolamine	p-cresol	1:1	
TRDES 6	Diethanolamine	m-cresol	1:1	
TRDES 7	Triethanolamine	o-cresol	1:1	
TRDES 8	Triethanolamine	p-cresol	1:1	
TRDES 9	Triethanolamine	m-cresol	1:1	
TRDES 10	Monoethanolamine	Guaiacol	1:1	
TRDES 11	Monoethanolamine	3-Methoxyphenol	1:1	[24]
TRDES 12	Monothanolamine	4-Methoxyphenol	1:1	
TRDES 13	2-(Methylamino)ethanol	Guaiacol	1:1	
TRDES 14	2-(Methylamino)ethanol	3-Methoxyphenol	1:1	
TRDES 15	2-(Methylamino)ethanol	4-Methoxyphenol	1:1	
TRDES 16	(Dimethylamino)ethanol	Guaiacol	1:1	
TRDES 17	(Dimethylamino)ethanol	3-Methoxyphenol	1:1	
TRDES 18	(Dimethylamino)ethanol	4-Methoxyphenol	1:1	
TRDES 19	L-menthol	Methyltriocetyl ammonium chloride	1:1	[25]
TRDES 20	L-menthol	Decanoic acid	1:1	
TRDES 21	L-menthol	Phenyl salicylate	1:1	
TRDES 22	L-menthol	Octanoic acid	1:1	

calculations, making the process highly time-consuming [28,29]. Therefore, a trimer of alginate was selected for the modelling, as this allows feasible quantum chemical calculations while still capturing the essential structural characteristics of the polymer [30,31].

With COSMO-RS, the activity coefficient of alginate was determined using Eqs. 1 and 2:

$$\ln(\gamma_i^\infty) = \frac{\mu_s^i - \mu_i^i}{RT} \quad (1)$$

$$\gamma_i^\infty = \lim_{xi \rightarrow 0} \gamma_i \quad (2)$$

where  $\gamma_i^\infty$  is the activity coefficient of alginate ( $i$ ) at infinite dilution, which is defined as the limiting value of the activity coefficient as the concentration of alginate approaches zero; it is determined based on the chemical potential of the solvent  $\mu_s$  and the chemical potential of the pure compound  $\mu^0$  [32,33].

The solubility capacity ( $C$ ) of each TRDES was calculated to determine the maximum amount of solute that can be dissolved in the TRDES, following Eq. 3 [33]:

$$C_i^\infty = 1/\gamma_i^\infty \quad (3)$$

The partition coefficient was calculated to evaluate the distribution of the solute between the DES and aqueous phases [34,35], providing insights into the alginate extraction and recovery efficiency. The partition coefficient was determined following Eq. 4:

$$K_{\text{water/DES}} = \frac{\frac{1}{\gamma_i^\infty(\text{water})}}{\frac{1}{\gamma_i^\infty(\text{DES})}} \quad (4)$$

**2.3.2.2. TRDES recycling simulation.** The partitioning behaviour of alginate across multiple extraction cycles was assessed by calculating the partition coefficient  $K_{\text{water/DES}}$  and through calculating the Gibbs free energy of transfer ( $\Delta G$ ) for the partitioning of alginate. This computational approach enables the evaluation of thermodynamic trends and insights into whether cumulative effects within the TRDES could account for the enhanced alginate release observed in later extraction cycles. The Gibbs free energy of transfer was calculated following Eq. 5:

$$\Delta G_{\text{Partitioning}} = -RT\ln(K_{\text{water/DES}}) \quad (5)$$

where  $R$  is the molar gas constant  $(8.314 \frac{J}{mol \cdot K})$  and  $T$  is the separation temperature ( $K$ ).

The recycling process was modelled using COSMO-RS to evaluate the partitioning behaviour of alginate over successive cycles. After each extraction cycle, it was assumed that 2 % of the total alginate accumulated in the DES phase. This retained alginate was then included in the solvent mixture composition for the subsequent cycle. At each stage, the updated solvent composition was used to recalculate the activity coefficient and partition coefficient of alginate.

#### 2.4. Alginate extraction and recovery

A TRDES-water system was prepared to achieve a 50 % v/v TRDES concentration [22], and this was used to extract alginate from *S. latissima* at a solid-to-total liquid ratio of 1:40. The extraction was performed at 60 °C for one hour in a water bath, with the solution vortexed every ten minutes to ensure thorough homogenisation.

As a control, water extraction was performed using the same conditions as applied with the TRDES extraction. Alkaline extraction was performed as a control for the conventional alginate extraction. For alkaline extraction, acidified water containing  $H_2SO_4$  (pH 1.9) was added to the seaweed at a 1:1 (w/w) ratio and incubated for one hour at room temperature. Subsequently,  $Na_2SO_4$  was added at a 0.0325:1 (w/w) ratio, followed by extraction for 1 h at 60 °C. All extractions, including those using different DESs and controls, were performed in triplicate.

Subsequently, the mixtures were centrifuged to separate the biomass residue. The supernatant was stored at 4 °C to facilitate phase separation between the aqueous and TRDES phases. Once phase separation occurred, the aqueous phase was collected and dialysed using a membrane with a molecular weight cutoff of 3.5–5 kDa. The alginate recovery yield of the dialysed aqueous phase was analysed using a colorimetric assay as proposed by Cesaretti et al. [36]. The alginate recovery yield was calculated following Eq. 6:

$$\text{Yield} \left( \frac{mg}{g \text{ DW}} \right) = \frac{C_{\text{aqueous}} * V_{\text{aqueous}}}{m_{\text{biomass}} * x_{\text{DW}}} \quad (6)$$

where  $C_{\text{aqueous}}$  is the concentration of the extract in the aqueous phase,  $m_{\text{biomass}}$  is the weight of the initial biomass,  $x_{\text{DW}}$  is the weight fraction of the dry biomass and  $V_{\text{aqueous}}$  is the volume of the aqueous phase.

The schematic diagram of the TRDES extraction and recovery

process is illustrated in Fig. 1.

## 2.5. Extraction optimisation

Extraction parameters were optimised with the best-performing DES (Section 2.4) to increase the alginate yield. The varied parameters include TRDES concentration (10 %–70 %), solid to total liquid ratio (1:40, 1:60, 1:80), extraction temperature (40–80 °C), and extraction time (10–60 min). When one parameter was varied, the others were kept constant according to the conditions in Section 2.4. These single-factor experiments follow an approach widely applied in literature focused on responsive solvents [37–39]. The obtained optimum extraction parameters were subsequently used in the TRDES recycling study.

## 2.6. TRDES and alginate characterisation

### 2.6.1. FTIR analysis

The TRDES, their individual components and alginate were analysed using Fourier-transform infrared (FTIR) spectroscopy. Spectra were recorded in the range of 400–4000 cm<sup>-1</sup> using a Nicolet Summit X ATR-FTIR spectrometer (Thermo Fisher Scientific).

For alginate, the extracts were isolated from the aqueous phase and purified by precipitation with 80 % ethanol containing 1 % NaCl, followed by two washes with 80 % ethanol. The resulting precipitate was dried under nitrogen and characterised using FTIR spectroscopy, Size Exclusion Chromatography (SEC) and for the mannuronic to guluronic acid (M/G) ratio. Extracts obtained using the conventional alkaline method and water extracts were compared with those from DES-based extraction.

### 2.6.2. Molecular weight

Size exclusion chromatography (SEC) was performed to analyse the molecular weight of alginate extracted with TRDES, water and alkaline extraction, as described previously [40]. Alginate solutions (0.15 % w/v) were prepared in Milli-Q water. A 20 µL sample was injected into an Agilent 1290 Infinity HPLC system equipped with two PL aquagel-OH MIXED-H columns (8 µm, 300 × 7.5 mm) in series. Elution was carried out using 0.1 M ammonium phosphate monobasic at pH 4.5 (Sigma-Aldrich) at a flow rate of 0.8 mL/min. Detection was performed with a refractive index detector (RID). A calibration curve was constructed using pullulan standards (PSS-PULKITR1, Agilent), and molecular weights were converted to alginate equivalents via the Mark-Houwink relation [40].

The average molecular weight ( $M_w$ ) was calculated following Eq. 7:

$$M_w = \frac{\sum (M_i^2 * c_i)}{\sum (M_i * c_i)} \quad (7)$$

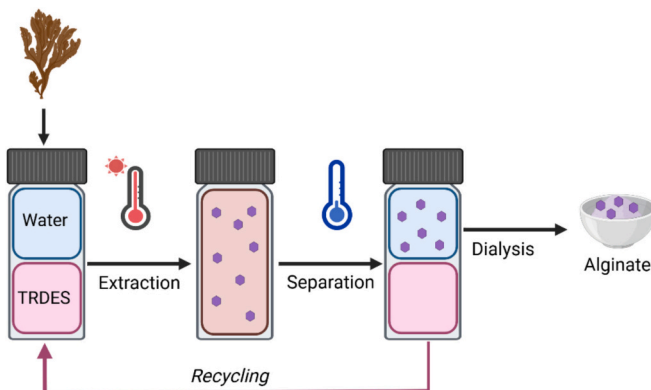


Fig. 1. Schematic diagram of alginate extraction using temperature-responsive deep eutectic solvents.

where  $M_i$  represents the molecular weight of fraction  $i$  corresponding to a specific retention time in the chromatogram, and  $c_i$  is the intensity (area) of fraction  $i$ , which is proportional to its concentration.

### 2.6.3. Mannuronic to guluronic acid ratio

The mannuronic to guluronic (M/G) ratio of the extracted alginate was analysed via methanolysis, followed by analysis using high-performance anion-exchange chromatography coupled with pulsed amperometric detection (HPAEC-PAD), following the methodology reported previously [41]. Measurements were performed on a Dionex ICS-6000 system (Thermo Fisher Scientific) equipped with a 1 mm CarboPac column. Alginate samples obtained via DES extraction were evaluated alongside those recovered through water extraction and conventional alkaline treatment. Prior to methanolysis, the samples were precipitated, redissolved in Milli-Q water, and 50 µL aliquots were used.

## 2.7. TRDES recycling

TRDES recycling was assessed after selecting the optimal TRDES formulation and optimal extraction conditions (Sections 2.4 and 2.5). The recycling capabilities of the TRDES were evaluated by repeating the same extraction procedure five times using the switched, recovered DES. The alginate recovery yield was measured in the aqueous phase after each extraction cycle.

## 2.8. Statistical analysis

Statistical analysis was performed using IBM SPSS Statistics version 30.0.0.0. The least significant difference (LSD) test and Duncan's multiple range test were applied to determine significant differences, with statistical significance set at  $p < 0.05$ . Error bars represent the standard deviation of three independent experiments. Different letters in the histogram indicate statistically significant differences at  $p < 0.05$ .

## 3. Results and discussion

### 3.1. TRDES phase behaviour

First, the 22 selected TRDES were assessed for their phase-switching ability. It was observed that alkanolamine:phenol-based TRDES (1 to 18) were immiscible with water at room temperature and became homogeneous mixtures with water when the solution was heated up to 60 °C (Table S1).

For TRDES 2–4, TRDES 10, and TRDES 12 and 16–18, phase separation occurred only upon cooling after adding 8 % sodium chloride. The addition of salt can enhance phase separation in TRDES systems, following a mechanism similar to salt-induced precipitation [24]. The less soluble component tends to precipitate out, while the more soluble component remains in the aqueous phase. In this case, sodium chloride is more soluble in water than the TRDES, promoting TRDES aggregation and separation from the aqueous phase at lower temperatures. In TRDES 10, incomplete phase separation occurred. An increased aqueous volume occurred after phase separation, indicating residual DES in the water. Therefore, it was discarded from further alginate extractions.

Out of the 22 TRDES, 17 could perform reversible phase separation. TRDES 10, 11, 13, 14 and 15 did not fully reverse during phase separation and were therefore discarded from the alginate extractions and partition behaviour.

### 3.2. Partition behaviour and extraction performance of alginate

#### 3.2.1. Computational analysis of capacity and partition coefficient

Prior to experimental extraction, COSMO-RS modelling was conducted to evaluate the capacity and partition coefficient ( $K_{\text{water/DES}}$ ) across the switchable TRDES systems for alginate. The capacity quan-

tifies the solute's ability to dissolve in the solvent, reflecting the extent of solute–solvent interactions. It is determined from the solute's activity coefficient, with lower activity coefficients indicating higher solubility within the DES. These thermodynamic parameters were used to estimate the potential effectiveness of each TRDES system and to predict the affinity of alginate for both the aqueous and DES phases. This computational analysis enabled the selection of TRDES candidates with favourable partitioning behaviour for subsequent experimental validation (Table 2).

In addition to calculating the activity coefficients ( $\gamma$ ) of the DES and water at 20 °C, the variation of the capacity and the partition coefficient (K) was also examined across a range of temperatures for each DES (Fig. 2, Fig. S3). This analysis was performed to investigate the influence on alginate partitioning when enabling temperature-responsive product recovery.

**3.2.1.1. Capacity.** The capacity of the TRDES–water systems for alginate decreased progressively from HBA monoethanolamine (31.5 for TRDES1) to diethanolamine (17.9 for TRDES4) and triethanolamine (12.9 for TRDES9) (Table 2). Monoethanolamine (MEA) based DES–water systems exhibited superior capacities due to their balanced hydrogen bonding capacity and favourable basicity [42]. Featuring both a primary amine ( $-\text{NH}_2$ ) and a hydroxyl ( $-\text{OH}$ ) group (Fig. S2), MEA can act as both a strong hydrogen bond donor and acceptor [43], enabling effective interactions with the carboxylate ( $-\text{COO}^-$ ) and hydroxyl ( $-\text{OH}$ ) groups of alginate (Fig. S1). Additionally, MEA's relatively high basicity ( $\text{pK}_a \sim 9.5$ ) compared to diethanolamine (DEA,  $\text{pK}_a \sim 8.7$ ) and triethanolamine (TEA,  $\text{pK}_a \sim 7.7$ ) [22,44] allows for partial protonation under aqueous conditions. The resulting  $-\text{NH}_3^+$  groups can engage in electrostatic interactions with negatively charged alginate, further enhancing affinity. In contrast, DEA and TEA contain secondary ( $-\text{NH}$ ) and tertiary ( $-\text{N}$ ) amines, respectively, which exhibit weaker hydrogen bonding capabilities and lower basicity, making MEA the most effective HBA in terms of capacity among the ethanolamines studied.

The DES–water (50:50) system exhibited significantly higher capacity than the DES without water (Table 2). This improvement is attributed to the role of water in increasing solvent polarity, enhancing hydrogen bonding, and reducing viscosity [45], which together promote more effective solvation of the alginate. In contrast, the DES without water offers limited capacity due to its lower polarity (Table S2) and higher viscosity compared to DES with water.

The menthol-based DES (TRDES19–22) with water showed low capacity toward alginate (less than 1.5) (Table 2). This could be due to their predominantly hydrophobic nature (Table S2), which reduces

**Table 2**

Capacities (C) and partition coefficients (K) of alginate in the TRDES–water systems at 20 °C.

	Capacity DES–water <sup>a</sup>	Capacity DES <sup>a</sup>	K <sub>Water/DES</sub> <sup>a</sup>
TRDES 1	$3.15 \times 10^1$	1.21	4.54
TRDES 2	$2.53 \times 10^1$	1.07	5.17
TRDES 3	$2.93 \times 10^1$	1.29	4.27
TRDES 4	$1.79 \times 10^1$	1.68	3.28
TRDES 5	$1.52 \times 10^1$	1.53	3.59
TRDES 6	$1.72 \times 10^1$	1.79	3.07
TRDES 7	$1.45 \times 10^1$	2.53	2.18
TRDES 8	$1.27 \times 10^1$	2.34	2.35
TRDES 9	$1.42 \times 10^1$	2.69	2.05
TRDES 12	$2.44 \times 10^1$	1.70	3.23
TRDES 16	$2.15 \times 10^1$	1.01	5.44
TRDES 17	$2.12 \times 10^1$	$3.26 \times 10^1$	$1.69 \times 10^{-1}$
TRDES 18	4.93	9.71	$5.68 \times 10^{-1}$
TRDES 19	$1.48 \times 10^3$	$1.85 \times 10^{-6}$	$2.97 \times 10^6$
TRDES 20	$5.36 \times 10^{-1}$	$3.29 \times 10^{-3}$	$1.67 \times 10^3$
TRDES 21	1.49	$8.28 \times 10^{-3}$	$6.66 \times 10^2$
TRDES 22	$7.07 \times 10^{-1}$	$5.73 \times 10^{-3}$	$9.62 \times 10^2$
Water	5.51		

<sup>a</sup> Calculations were performed at 20 °C.

their solvation capacity toward alginate.

**3.2.1.2. Partition coefficient.** When considering the partition coefficient, it can be observed that the partition coefficient is above 0 for all TRDES at 20 °C (Table 2) and across 20–80 °C (Fig. 2 and Fig. S3). This indicates that alginate prefers partitioning into the water phase over the DES phase at all temperatures for each DES.

Additionally, the partition coefficient decreased at higher temperatures for each TRDES (Fig. S3). For TRDES1, this decrease is from approximately 4.54 at 20 °C to 0.88 at 80 °C (Fig. 2), suggesting that alginate is more likely to partition into the water phase at lower temperatures. This indicates that temperature affects the relative solubility of alginate in the two phases, with lower temperatures enhancing its distribution toward water. This is desirable, as TRDES–water phase separation occurs at 20 °C, making it convenient for efficient partitioning of alginate into the aqueous phase.

For TRDES 18–22, the partition coefficient was significantly larger than 1 at 20–80 °C (Table 2, Fig. 2 and Fig. S3), indicating that alginate preferentially partitions in the water phase over the DES phase. Due to the hydrophobicity of these DESs (Table S2), they exhibit poor compatibility with alginate, as indicated by the low capacities. This, in turn, results in minimal solubilisation within the DES phase and thus good separation ability.

Since all TRDES showed a positive partition coefficient at 20 °C and demonstrated moderate to good capacities, these DESs were considered for laboratory alginate extraction.

### 3.2.2. Experimental evaluation of alginate extraction yields

All of the TRDESs that could undergo phase separation recovered alginate in the aqueous phase (Fig. 3). The highest yield was obtained by TRDES 1 (ethanolamine:o-cresol 1:1) and TRDES 16, which recovered  $25.0 \pm 3.6$  and  $23.6 \pm 4.2$  mg/g DW, respectively, in their aqueous phase (Fig. 3). Compared to water extraction, TRDES 1 and 16 resulted in a two-times higher alginate yield, which could be due to the higher capacities of these DESs compared to water due to their improved hydrogen bonding capacities (Section 3.2.1).

In general, it was observed that the alkanolamine: phenol-based DES could recover more alginate than the menthol-based DES (TRDES 19–22) (Fig. 3). This may be attributed to the mildly alkaline conditions created by the alkanolamine–phenol-based DES [22]. Since the  $\text{pK}_a$  of an alginate polymer is in the range of 3.5–4.6 [46], this causes alginate to dissolve in alkaline conditions. The increased yield compared to the menthol-based DES is consistent with the computationally obtained capacities (Section 3.2.1).

Differences among yields for alkanolamine: phenol-based DES could be due to the interaction between the DES and biomass. In addition to solute–solvent affinity, the capacity of DES to alter biomass structure by modulating cell membrane permeability and compromising structural integrity also contributes to its extraction performance [47–49]. This, in turn, can affect the accessibility of alginate and may significantly influence the extraction efficiency. Specifically, previous studies have demonstrated that certain TRDESs and DESs can alter the permeability and integrity of plant and microalgal cell walls, thereby enhancing the release of target compounds [25,50].

Alkaline extraction reached a yield of  $42.1 \pm 3.7$  mg/g DW. Despite the lower yield of TRDES 1 and 16 compared to alkaline extraction, TRDES extraction could offer advantages in process intensification and process circularity. Extraction with TRDES enables the simultaneous extraction and separation of product and DES in a single one-hour step, compared to two one-hour steps for alkaline extraction. In addition, TRDES extraction allows for direct alginate recovery from the aqueous phase. Furthermore, TRDES allow for the recycling of the extraction solvent, thereby enhancing its sustainability.

TRDES 1 was selected for further optimisation due to its high solubility capacity and favourable partition coefficient

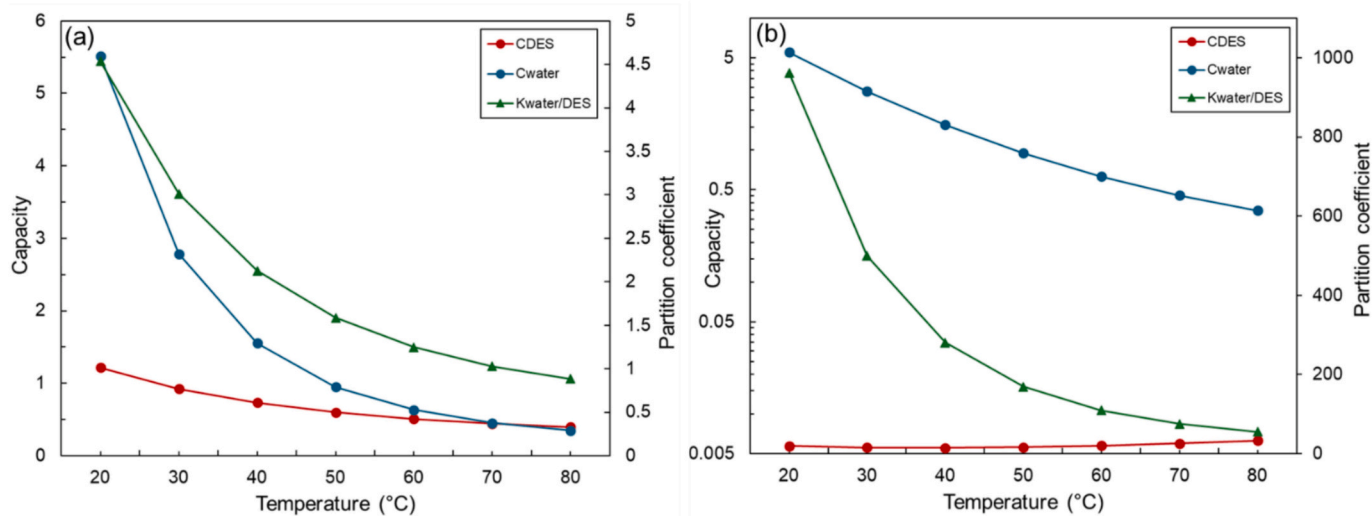


Fig. 2. Capacity and partition coefficient (K) of (a) TRDES1 with water and (b) TRDES20 with water as a function of temperature (20–80 °C).

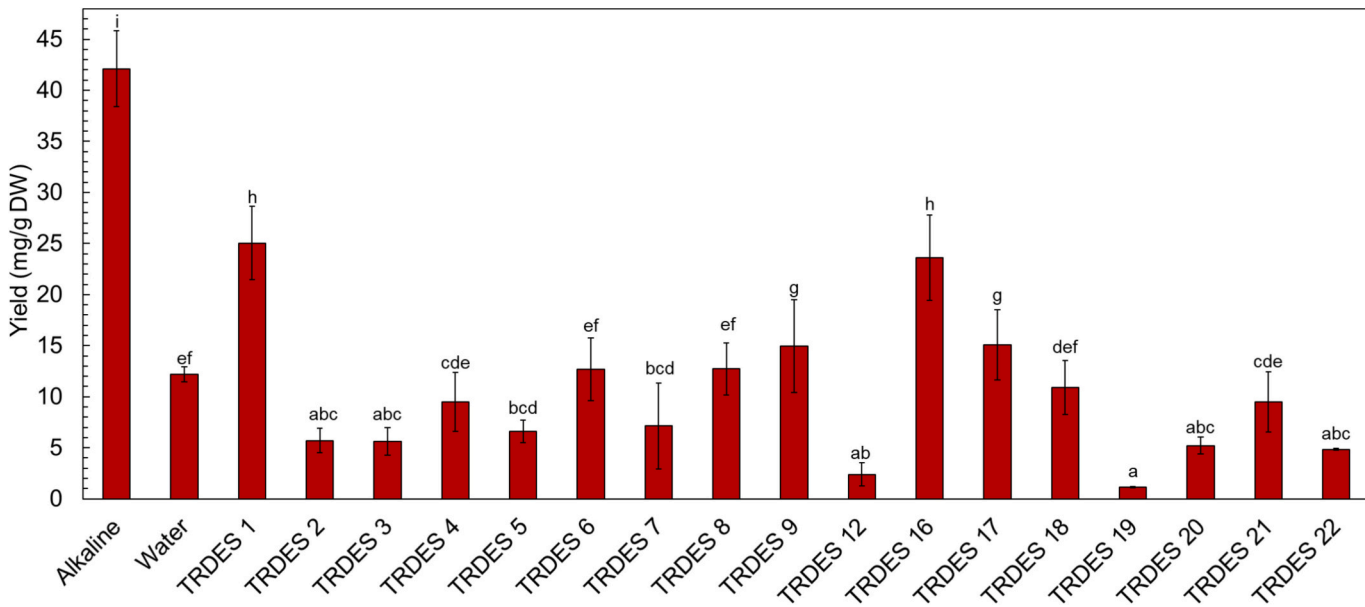


Fig. 3. Alginate extraction yield for TRDES-water systems for TRDES1–TRDES22. Extraction with only water and alkaline extraction were used as controls.

### 3.3. Extraction parameters

From the previous section (Section 3.2), TRDES 1 was selected for extraction optimisation. Optimisation was performed to identify the impact of extraction parameters on the alginate yield. In this study, TRDES concentrations, solid to total liquid ratio, extraction temperature and extraction time were investigated to enhance alginate recovery yield (Fig. 4). Single-factor experiments were employed to evaluate the effect of each parameter independently, an approach widely applied and effective in responsive solvent optimisation studies [37–39].

#### 3.3.1. Effect of extraction temperature

The influence of extraction temperature on the alginate recovery yield was examined from 40 to 80 °C. The extraction yield increased as the temperature increased (Fig. 4a). The UCST of TRDES1 is 55 °C [22], indicating that a homogeneous solution forms above 55 °C, where TRDES1 becomes fully miscible with water. Consequently, a marked difference in alginate yield is observed when comparing extraction

temperatures below the UCST (50 °C, 10.2 ± 3.3 mg/g DW) and above it (60 °C, 23.0 ± 2.6 mg/g DW). Below the UCST, a heterogeneous system is formed because TRDES is insoluble in water, which impairs mass transfer and molecular diffusion [51]. Above the UCST, TRDES1 becomes fully miscible with water and forms micelle-like aggregates [22]. This arises from the amphiphilic nature of its components: monoethanolamine provides polar headgroups capable of hydrogen bonding, while o-cresol contributes hydrophobic aromatic moieties (Fig. S2). Elevated temperatures increase molecular mobility and weaken hydrogen bonding, allowing the amphiphilic molecules to self-assemble into micelles. These structures create localised microenvironments of differing polarity, enhancing alginate solubilisation and mass transfer [22]. Below the UCST, partial phase separation suppresses micelle formation, resulting in a heterogeneous system with limited diffusion and reduced extraction efficiency. Additionally, elevated temperatures can promote the rupture of the cell wall [52], thereby enhancing alginate release. Therefore, 80 °C was selected as the optimal temperature.

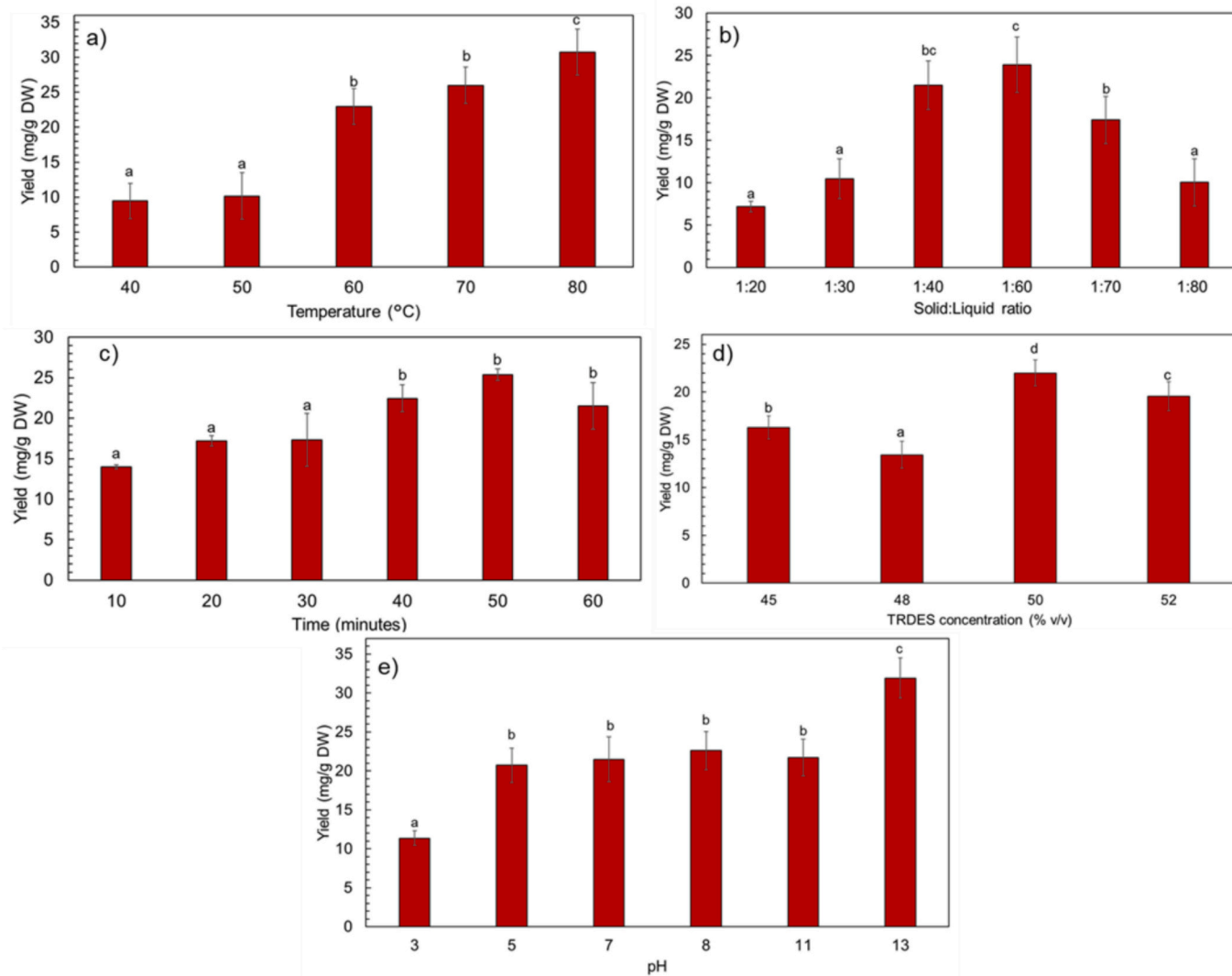


**Fig. 4.** Effect of (a) the extraction temperature, (b) the solid:liquid ratio, (c) the extraction time, (d) the TRDES concentration and (e) the pH on the alginic acid extraction yield. Conditions were standardised at 60 °C, solid:liquid ratio of 1:40, one hour extraction time, at 50 % v/v TRDES concentration and pH 7 of the water when one of the extraction parameters was altered.

### 3.3.2. Effect of solid-liquid ratio

Solid-liquid ratios from 1:20 to 1:80 (g/mL) were assessed. The results show that from 1:20 to 1:60, the alginic acid yield increases and then decreases when further increasing the solid-liquid ratio (Fig. 4b). The extraction yield increased noticeably with an increase in the liquid-solid ratio. A higher concentration of extractant enhances the dissolution of target compounds into the extraction medium due to improved mass transfer [53], thereby increasing the yield from 7.2 ± 0.6 to 23.0 ± 3.3 mg/g DW when using 1:20 and 1:60 solid-liquid ratios, respectively. However, an excessive amount of extractant not only adversely affects the extraction efficiency but may also lead to resource waste [24,54,55]. Therefore, a solid-liquid ratio of 1:60 was selected.

### 3.3.3. Effect of extraction time

The extraction time of 10 to 60 min was examined. The alginic acid yield increased up to 40 min, but extracting longer than 40 min did not significantly affect the extraction yield (Fig. 4c). This initial increase is due to the progressive diffusion of alginic acid into the extraction solvent. During the early stages of extraction, the concentration gradient between the polysaccharide in the biomass and the solvent is high, which promotes mass transfer [56]. However, beyond 40 min, the extraction yield plateaus, which could be due to the accumulation of impurities

[57] or because the extraction process has reached equilibrium [58]. Therefore, 40 min was chosen as the optimal extraction time.

### 3.3.4. TRDES concentration

The TRDES concentration of 45 to 52 % was investigated for alginic acid extraction. The optimal yield was obtained when having a 50 % TRDES concentration, and increasing or decreasing the concentration resulted in lower yields (Fig. 4d). At lower TRDES concentrations, the solvent may be too diluted, reducing its ability to break down the cell structure [22], which will in turn result in less alginic acid release. Additionally, lower TRDES concentrations can weaken the interactions between the solvent and alginic acid. At higher TRDES concentrations, the viscosity of the mixture increases, which can hinder mass transfer and diffusion of target compounds into the solvent phase [54,59]. Therefore, a 50 % TRDES concentration was selected as the optimal condition.

### 3.3.5. Effect of pH

The pH value of the water was adjusted from pH 3 to pH 13. The extraction yield increased when the pH was increased (Fig. 4e). This improved yield when elevating the pH could be because the pKa of an alginic acid polymer is in the range of 3.5–4.6 [46,60], which makes alginic acid dissolve in alkaline conditions. On the other hand, acidic conditions

promote the protonation of carboxyl groups in alginate, leading to polymer precipitation or gel formation, thereby limiting its solubility [61], resulting in a decreased extraction yield. Therefore, pH 13 was selected as the optimal pH value. Although this pH falls within the alkaline range, this treatment fundamentally differs from conventional extraction, as no concentrated sulfuric acid is used and the process occurs in a single step. Moreover, the TRDES can be recovered and reused, reducing reagent consumption compared to traditional alkaline extraction.

### 3.4. TRDES and alginate characterisation

Based on the optimal conditions identified in [Section 3.2](#), the subsequent extraction was performed based on these conditions and characterisation of both the extracted alginate and the DES was performed.

#### 3.4.1. TRDES characterisation

To confirm the temperature-responsive behaviour of the DES system, TRDES1 was characterised across the phase transition temperature with FTIR ([Fig. 5](#), [Table S3](#)). This evaluation aimed to verify the reversible switching of the DES between biphasic and monophasic states.

For ethanolamine, the FTIR spectrum typically shows a broad O–H/N–H stretching band around 3000–3400 cm<sup>–1</sup> and distinct C–N stretching near 1075 cm<sup>–1</sup> [62].

For o-cresol, characteristic peaks include aromatic C=C stretching at approximately 1600 cm<sup>–1</sup>, and C–O stretching near 1200 cm<sup>–1</sup> [63]. Upon DES formation, a small peak is observed at 3344 cm<sup>–1</sup> corresponding to hydrogen bonding interactions between ethanolamine and o-cresol, consistent with previous reports [22]. Upon the addition of water to the DES and heating, a broader band emerges at 3400 cm<sup>–1</sup>, indicating the formation of additional hydrogen bonds between water molecules and the DES components [22]. In addition, the aqueous phase obtained after switching was analysed ([Fig. S4](#)). The FTIR spectrum of this water phase was compared to that of pure water. No distinct peaks attributable to DES components were observed, suggesting the absence of detectable DES traces in the aqueous phase ([Fig. S4](#)).

#### 3.4.2. Alginate characterisation

The alginate recovered from the TRDES was characterised for its functional groups with FTIR, for its molecular size and the M/G ratio.

The FTIR spectra of alginate extracted using DES, water and alkaline treatment exhibited comparable profiles ([Fig. 6](#), [Table S4](#)), with characteristic absorption bands observed at 1080 cm<sup>–1</sup> and 1020 cm<sup>–1</sup>, corresponding to vibrations of guluronic and mannuronic acid residues, respectively [64,65]. The bands at ~1600 cm<sup>–1</sup> and ~1400 cm<sup>–1</sup> are attributed to the asymmetric and symmetric stretching vibrations of the carboxylate (–COO<sup>–</sup>) functional groups, respectively [65–67]. Additionally, a broad absorption band around 3500 cm<sup>–1</sup> and a weak band near 2900 cm<sup>–1</sup> were observed, corresponding to hydrogen-bonded O–H stretching and C–H stretching vibrations, respectively, present in alginate [66].

The molecular weights of alginate extracted using TRDES (989 ± 227 kDa) and conventional alkaline extraction (988 ± 21 kDa) were similar, indicating comparable average molecular sizes ([Fig. 7](#)). In contrast, water-extracted alginate had a significantly lower molecular weight (445 ± 71 kDa). The comparable molecular weights observed for TRDES and conventional alkaline extraction suggest that TRDES is an effective alternative for alginate extraction and recovery, achieving alginate with similar molecular weights.

The mannuronic to guluronic (M/G) ratio is an important parameter in alginate characterisation, as it determines the polysaccharide's structural, physical, and functional properties [41]. Alginate gels with a high M/G ratio tend to exhibit greater permeability, while those with a low M/G ratio typically form more robust and rigid networks. The G-blocks exhibit greater rigidity due to the increased restriction of rotational freedom around their glycosidic linkages, promoting tighter cross-linking and improved mechanical strength compared to gels rich in mannuronic acid blocks [68,69].

Alginate extracted with TRDES resulted in an M/G ratio of 2.63 ± 0.19, while for alkaline and water this was 1.15 ± 0.01 and 1.55 ± 0.02, respectively ([Table 3](#)). The M/G ratios obtained from TRDES extracts were higher than those from conventional alkaline extraction methods and also exceeded the values reported in the literature for *Saccharina latissima*, ranging from 0.8 to 1.49, depending on the extraction method [41,70,71]. The higher M/G ratio could be because the TRDES extraction was performed at higher pH conditions, causing an increased M/G ratio [70]. This effect may be attributed to partial degradation of alginate under alkaline conditions, coupled with differences in the solubility of the resulting shorter polymer fragments depending on their uronic acid composition. This indicates that alginate extracted using TRDES

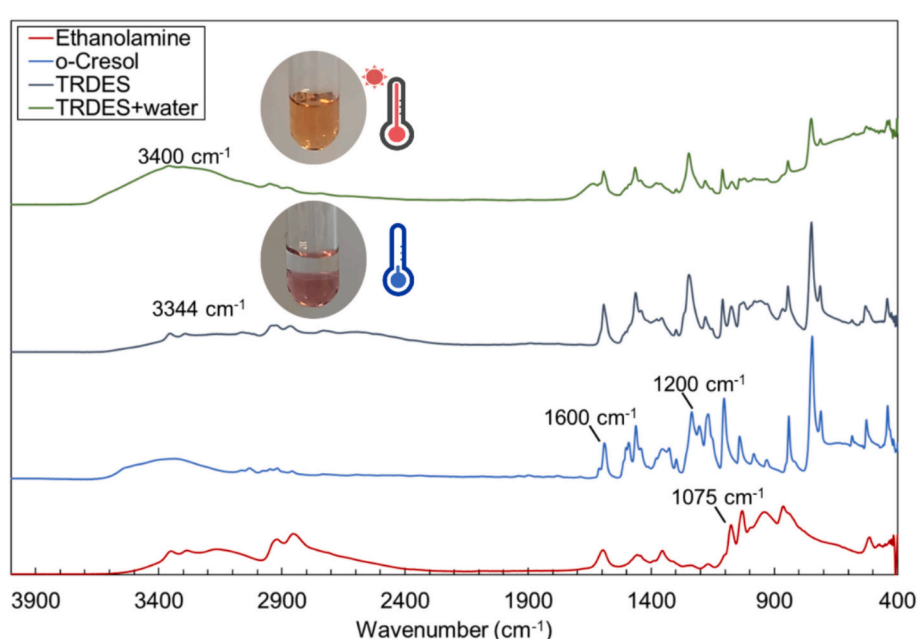


**Fig. 5.** FTIR spectra of TRDES1 constituents, TRDES1 and TRDES1 containing 50 %v/v water.

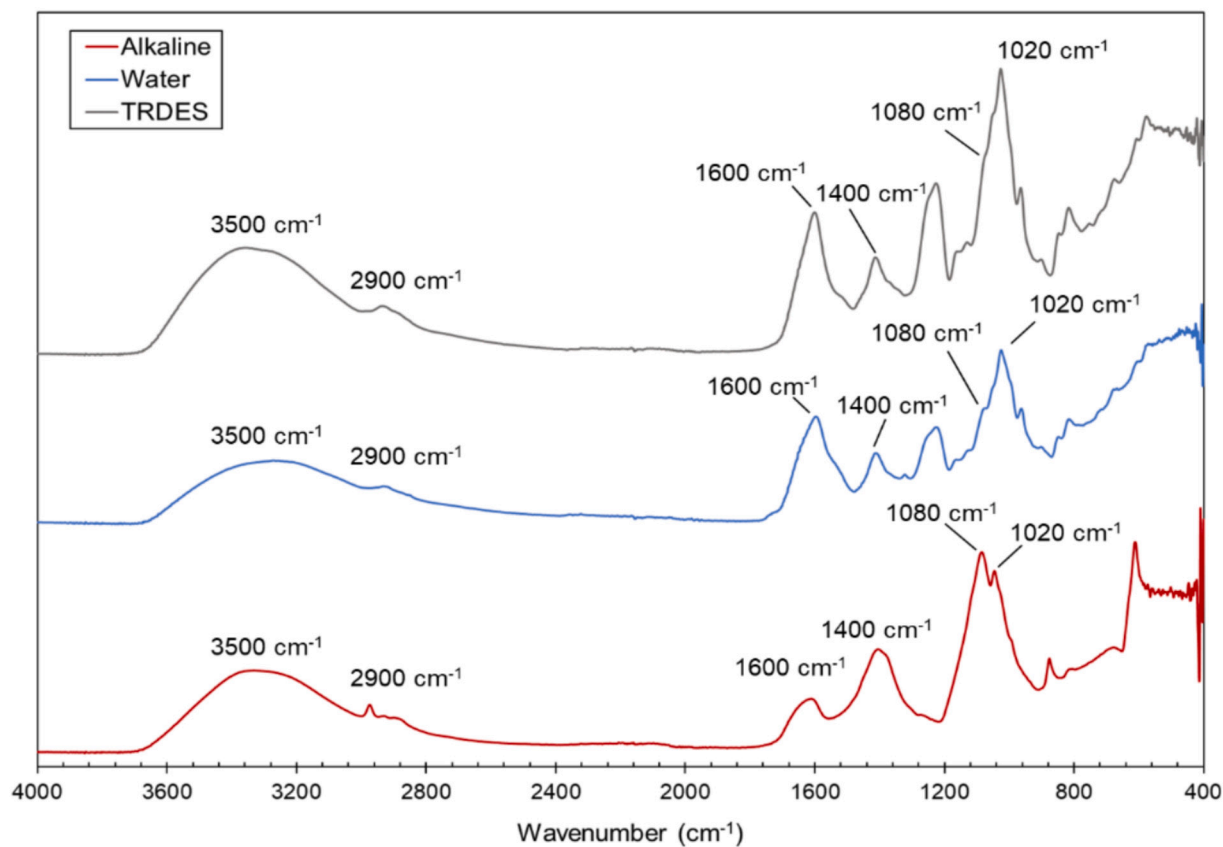


Fig. 6. FT-IR spectra of alginate extracted with TRDES, conventional alkaline processing and with water.

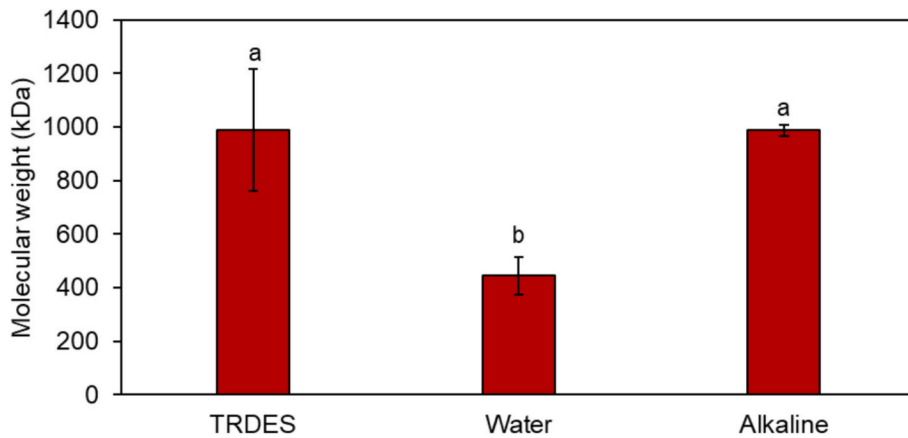


Fig. 7. Molecular weight of alginate extracted with TRDES, water and alkaline treatment.

**Table 3**  
M/G ratios of alginate extracted with TRDES, conventional alkaline treatment and water.

	M/G ratio
TRDES	2.63 ± 0.19
Alkaline	1.15 ± 0.01
Water	1.55 ± 0.02

may yield more flexible, elastic, and permeable gel networks compared to alginate recovered through alkaline treatment. Such properties make this alginate particularly suitable for diffusion-dependent applications, including drug delivery systems and cell encapsulation technologies.

Based on FTIR, molecular size, and M/G ratio data, TRDES and

conventional alkaline extraction yielded alginate with comparable molecular characteristics. However, TRDES could offer additional advantages due to its potential for recyclability, positioning it as a more circular alternative.

### 3.5. TRDES recycling

The recyclability of the TRDES solvent was evaluated to assess its feasibility for repeated extraction of alginate. Eight extraction cycles were performed using the same solvent to determine the impact of recycling on extraction efficiency and solvent performance. The recycling study was conducted under the optimum extraction conditions determined previously (Section 3.3).

The extraction yield of TRDES 1 remained stable from cycle 1 to 4

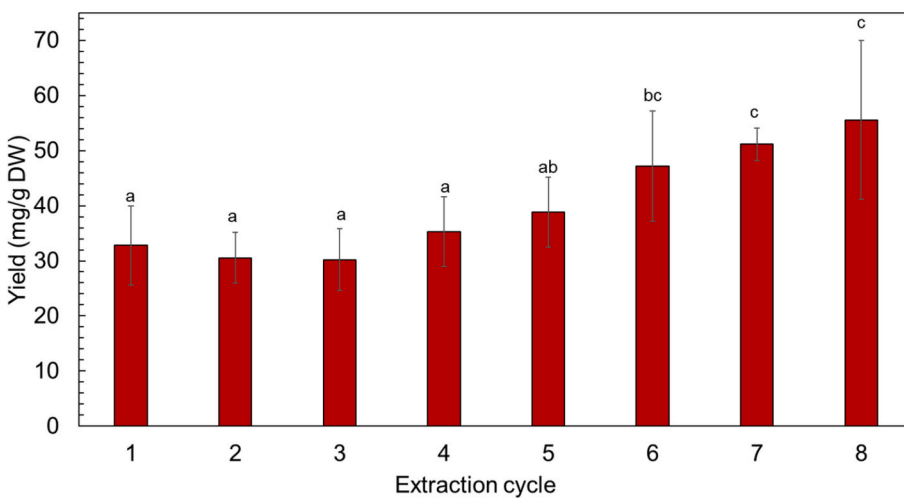


Fig. 8. Extraction yield of alginate obtained using TRDES1 over eight consecutive recycling cycles.

(Fig. 8). Starting from cycle 4, an increase in extraction yield was observed, with an extraction yield of  $55.6 \pm 14.4$  mg/g DW at cycle 8. From cycle seven to eight, no statistically significant difference in extraction yield was observed, suggesting that the system may have approached a plateau. The larger standard deviation in the final cycle is attributed to variability between experimental replicates and analytical uncertainty, rather than incomplete phase separation or reduced solvent performance. A previous study on alginate extraction using the hydrophilic DES betaine:urea reported a recovery of  $56.0 \pm 0.9$  mg/g, achieved through a two-step aqueous two-phase system (ATPS) [72]. In that process, alginate first partitioned into a copolymer-rich phase, after which both the copolymer and DES phases had to be separated and recycled. A second ATPS step was then required to transfer alginate into the aqueous phase while recovering the copolymer for reuse. Although the final yields are comparable to those obtained in our study, the ATPS method involves multiple sequential separation and recycling steps. By contrast, our TRDES-based process combines extraction and solvent recovery in a single step, offering a simpler and potentially more efficient alternative. In another study, Saravana et al. [73] used subcritical water extraction at  $125^\circ\text{C}$  and 10 bar with a choline chloride:glycerol (1:2) DES containing 70 % water, obtaining an alginate yield of 28 %, indicating similar extraction yields compared with our study (approximately 33 %). While effective, this method did not include DES recycling and relies on high-pressure equipment, which can increase capital costs.

When comparing DES recycling to other studies, Ng et al. [74] reported that during the extraction of ferulic acid from oil palm empty fruit bunch fibre, the addition of an antisolvent enabled ferulic acid precipitation. Using this approach, they were able to recycle the DES for up to five consecutive cycles without significant loss of performance. Chen et al. [75] used  $\text{CO}_2$ -triggered switchable hydrophilicity solvents for ultrasonic-assisted extraction of *Polygonatum sibiricum* polysaccharides. The solvent could be recycled five times, observing a decrease in extraction yield per cycle. Gao et al. [76] et al. performed oil extraction from sawdust. The hydrophobic DES was regenerated through deprotonation and protonation using NaOH and acetic acid, respectively. They found a significant decrease in extraction efficiency upon recycling a hydrophobic DES five times. Compared with other DES recycling strategies, the proposed TRDES system supports a higher number of successful recycling cycles, as the recovery yield continues to increase rather than decline over successive rounds.

The trend of an increase in the extraction yield contrasts with previous TRDES recycling studies, where extraction efficiencies declined with successive cycles [22,25]. In these studies, the accumulation of other constituents in the DES could have competed with the target

compound [74], thereby reducing the solvents' effectiveness. However, other studies focused on DES recycling have found increasing extraction yields, as observed for alginate, due to compound accumulation in the DES phase [74]. The sustained and improved performance observed here may be attributed to the accumulation of alginate in the DES phase, resulting from the moderate affinity that the DES has for alginate (Table 2).

The increase in extraction yield could thus be due to incomplete phase separation of alginate into the aqueous phase in the previous cycles, due to the carryover of alginate that remains solubilised within the TRDES during cycles 1–4. During the first cycles, part of the alginate may remain dissolved in the TRDES phase as the optimal partitioning equilibrium has not yet been reached. As the TRDES system is reused, the TRDES could reach saturation. This accumulation, in turn, could influence the partition coefficient. Previous work by Cai et al. [22] stated a polysaccharide recovery yield of 88 % from *Ganoderma lucidum*, indicating that part of the alginate could be retained as well in the TRDES.

To establish a theoretical framework supporting the hypothesis of potential alginate accumulation within the TRDES phase, COSMO-RS modelling was employed. The partitioning behaviour of alginate across multiple extraction cycles was assessed, incorporating an assumption that 2 % of alginate remained accumulated in the DES phase after each cycle. This iterative approach allowed simulation of progressive enrichment of alginate in the DES, enabling evaluation of its impact on the partition coefficient and the Gibbs free energy of transfer ( $\Delta G$ ) (Section 2.3.2.2).

The COSMO-RS modelling results showed a progressive increase in the partition coefficient and a corresponding decrease in the Gibbs free energy of transfer ( $\Delta G$ ) over successive extraction cycles, while having a reduction in solubility capacity (Fig. 9, Table S5), indicating an increasing thermodynamic favourability for alginate partitioning into the aqueous phase. By cycle 8,  $\Delta G$  becomes negative, indicating a spontaneous transfer of alginate from the DES to the water phase. This trend suggests a reduction in alginate solubility within the DES, likely due to the potential accumulation of alginate in the DES phase across cycles, leading to saturation. As a result, the driving force for alginate transfer into the aqueous phase increases and the partition coefficient increases (Fig. 9). These computational findings are consistent with the experimentally observed increase in extraction yield upon solvent reuse (Fig. 8). The observed changes in partitioning behaviour may diminish the DES its solvation capacity for alginate, thereby enhancing its release into the aqueous phase.

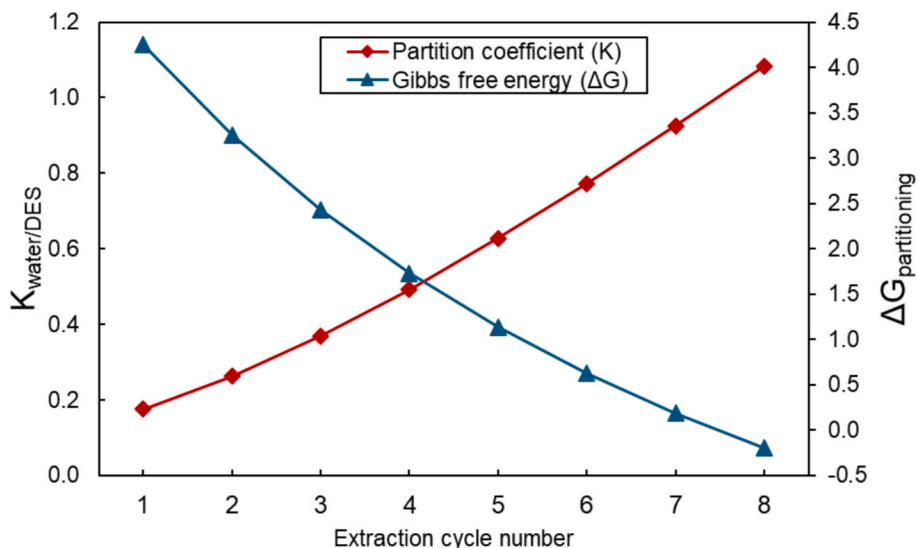


**Fig. 9.** Partition coefficient and Gibbs free energy of transfer when recycling TRDES1 eight times, assuming 2 % accumulation of alginate in the TRDES phase per extraction cycle.

### 3.6. Design criteria for novel TRDES

Temperature-responsive deep eutectic solvents (TRDES) effectively extracted alginate with considerable yields while enabling solvent recycling. Both COSMO-RS analysis and experimental data highlighted that the main solvent features governing extraction efficiency and recyclability are the capacity, partition coefficient and the Gibbs free energy of transfer. The capacity (C) of the TRDES-water system should exhibit moderate capacity (10–30), thereby allowing extraction, while the capacity of the sole TRDES should be low (< 1.2), promoting alginate recovery from the TRDES. The partition coefficient (K) should be above 1 at room temperature, so that the compound favours the aqueous phase upon switching, indicating that the TRDES facilitates effective compound recovery. Trends in the Gibbs free energy of transfer ( $\Delta G$ ) across successive recycling cycles revealed that gradual accumulation of alginate enhances its partitioning into water. Together, these observations suggest that solvents with moderate affinity are optimal for balancing extraction performance with efficient recovery and recyclability.

Although the alkanolamine-phenol-based TRDES1 delivered high alginate yields with functional properties and stable recycling, these are potentially hazardous compounds. In contrast, menthol-based solvents (TRDES19–22) are non-toxic but show lower capacity. This highlights a critical design challenge: achieving effective extraction and favourable partitioning from water without relying on hazardous solvent constituents. In this study, the primary objective was therefore to gain mechanistic insights into their behaviour upon recycling. These insights guide the future development of greener, more biocompatible TRDES systems. Currently, no recyclable TRDES based on natural, non-toxic components have been reported, limiting their applicability as truly green solvents. Zhang et al. [77] applied a biphasic natural TRDES system composed of decanoic acid: octanoic acid (1:2) and choline chloride: levulinic acid (1:2) for extracting bioactives from *Zanthoxylum bungeanum* peels. Although lowering the temperature successfully induced phase separation of the two DES, the target bioactives still required recovery using macroporous resins. This additional step washed out the DES phase, preventing solvent recycling and thereby undermining the main advantage of the TRDES concept. Similarly, Wang et al. [53] designed a DES/ionic liquid/water system using natural DES. While they successfully separated rosmarinic acid and carnosic acid into distinct DES- and ionic liquid-rich phases, the compounds remained dissolved in their respective solvents, impairing the recyclability of DES and reducing the

primary advantage of TRDES. This highlights the need for natural TRDES that enable product recovery and solvent recycling solely via temperature modulation. As an alternative, it would be interesting to explore LCST-type TRDES for future solvent design. LCST systems separate upon heating because hydrophobic interactions become dominant at elevated temperatures, disrupting hydrogen bonding with water [21,54].

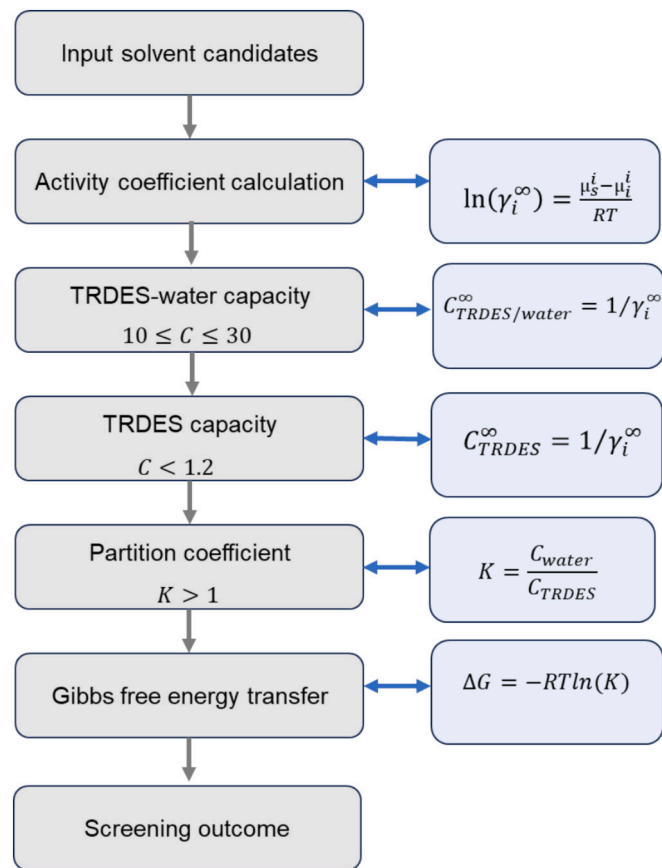


**Fig. 10.** Process overview for designing natural TRDES for circular, green solvent extraction. (For interpretation of the references to colour in this figure legend, the reader is referred to the web version of this article.)

For future research, it is recommended to select natural HBAs and HBDs exhibiting moderate hydrophobicity, and perform computational solvent pre-screening (capacity, partition coefficient and Gibbs free energy change) to choose suitable candidates (Fig. 10). Recent advances in machine-learning-enhanced COSMO-RS workflows offer an additional opportunity to accelerate this process [78]. ML models trained on quantum-chemical descriptors can rapidly predict key solvent properties across large chemical spaces, enabling more efficient identification of promising natural TRDES candidates before experimental validation.

By modelling water-DES phase behaviour (UCST/LCST), their switchability can be assessed, followed by experimental phase behaviour assessment. Combining this data should give preferred candidates for laboratory validation on extraction, switching and solvent recycling (Fig. 10). Focusing on natural compounds for designing temperature-switchable DES, supported by ML-accelerated screening, not only enhances process intensification compared to conventional DES extraction but also contributes to greater sustainability. This combined computational-experimental strategy facilitates the development and integration of DES technologies within biorefinery applications, promoting greener and more efficient biomass valorisation.

#### 4. Conclusion

This study demonstrated the feasibility of temperature-responsive deep eutectic solvents (TRDES) as recyclable media for alginate extraction from *Saccharina latissima*. Initial solvent screening, supported by COSMO-RS modelling, identified TRDES1 as the most effective system. Under optimised conditions, TRDES1 enabled functional alginate extraction and was successfully recycled for eight consecutive cycles, with yields progressively increasing to  $55.6 \pm 14.4$  mg/g DW. Thermodynamic modelling confirmed that this behaviour is linked to changes in alginate partitioning, with increasing partition coefficients across cycles, reflecting enhanced favourability for alginate recovery upon reuse.

Experimental data and COSMO-RS analysis showed that the capacity, partition coefficient, and Gibbs free energy of transfer were identified as the main factors influencing TRDES performance. Optimal extraction, partitioning and recyclability can be achieved with moderate TRDES-water capacity (10–30), low TRDES capacity (<1.2), and partition coefficients above 1. These findings establish preliminary design rules for future solvent development, emphasising the importance of moderate affinity to balance extraction efficiency and recovery potential.

However, the current well-performing TRDES are based on alkanolamine-phenol combinations, which limit environmental sustainability due to toxicity concerns. Bridging this performance-sustainability gap requires the development of natural TRDES composed of amino acids, sugars, and organic acids, ideally exhibiting LCST-type behaviour. To further extend the scope of this research, future work should integrate COSMO-RS with emerging machine-learning frameworks to accelerate the discovery of greener, biocompatible TRDES. ML-enhanced predictive models can rapidly screen large chemical spaces, identify promising natural HBA/HBD combinations, and guide the rational design of switchable, recyclable solvents. By uniting mechanistic understanding, thermodynamic criteria, and data-driven predictive tools, this study lays the foundation for developing non-toxic TRDES tailored for circular and sustainable biorefinery applications.

#### CRediT authorship contribution statement

**Isa S.A. Hiemstra:** Writing – original draft, Visualization, Validation, Methodology, Investigation, Formal analysis, Data curation, Conceptualization. **Faridah Husna:** Methodology, Investigation, Data curation. **Michel H.M. Eppink:** Validation, Supervision. **Rene H. Wijffels:** Validation, Supervision. **Antoinette Kazbar:** Supervision,

Resources, Project administration, Funding acquisition, Conceptualization.

#### Declaration of competing interest

The authors declare that they have no known competing financial interests or personal relationships that could have appeared to influence the work reported in this paper.

#### Acknowledgements

This work was funded by the Dutch Research Council (NWO) (The Hague, NL) under the SeaSolv project (<https://app.dimensions.ai/details/grant/12924032>). Grant number 19479.

#### Appendix A. Supplementary data

Supplementary data to this article can be found online at <https://doi.org/10.1016/j.seppur.2026.136807>.

#### Data availability

Data will be made available on request.

#### References

- A. Akter, M.K.A. Sobuj, M.S. Islam, K. Chakraborty, N. Tasnim, M.H. Ayon, M. F. Hossain, S.M. Rafiquzzaman, Seaweed polysaccharides: sources, structure and biomedical applications with special emphasis on antiviral potentials, Future Foods 10 (2024), <https://doi.org/10.1016/j.fufo.2024.100440>.
- A. Sadeghi, A. Rajabian, N. Nabizade, N. Meygoli Nezhad, A. Zarei-Ahmady, Seaweed-derived phenolic compounds as diverse bioactive molecules: a review on identification, application, extraction and purification strategies, Int. J. Biol. Macromol. 266 (2024), <https://doi.org/10.1016/j.ijbiomac.2024.131147>.
- Celente G. de Souza, Y. Sui, P. Acharya, Seaweed as an alternative protein source: prospective protein extraction technologies, Innov. Food Sci. Emerg. Technol. 86 (2023), <https://doi.org/10.1016/j.ifset.2023.103374>.
- H. Wang, L. Yang, Y. Yang, A review of sodium alginate-based hydrogels: structure, mechanisms, applications, and perspectives, Int. J. Biol. Macromol. 292 (2025), <https://doi.org/10.1016/j.ijbiomac.2024.139151>.
- T.A. Fenorodosoa, G. Ali, C. Delattre, C. Laroche, E. Petit, A. Wadouachi, P. Michaud, Extraction and characterization of an alginate from the brown seaweed *Sargassum turbinarioides* Grunow, J. Appl. Phycol. 22 (2010) 131–137, <https://doi.org/10.1007/s10811-009-9432-y>.
- S. Saji, A. Hebdon, P. Goswami, C. Du, A brief review on the development of alginate extraction process and its sustainability, Sustainability (Switzerland) 14 (2022), <https://doi.org/10.3390/su14095181>.
- M.Á. de los Fernández, J. Boiteux, M. Espino, Gomez FJV, M.F. Silva, Natural deep eutectic solvents-mediated extractions: the way forward for sustainable analytical developments, Anal. Chim. Acta 1038 (2018) 1–10, <https://doi.org/10.1016/j.aca.2018.07.059>.
- B.B. Hansen, A. Horton, B. Chen, D. Poe, Y. Zhang, S. Spittle, J. Klein, L. Adhikari, T. Zelovich, B.W. Doherty, B. Gurkan, E. Maginn, A. Ragauskas, M. Dadmunt, T. Zawodzinski, G.A. Baker, M. Tuckerman, R.F. Savinell, J.R. Sangoro, Deep Eutectic Solvents: A Review of Fundamentals and Applications, 2020, <https://doi.org/10.1021/acs.chemrev.0c00385>.
- E.L. Smith, A.P. Abbott, K.S. Ryder, Deep eutectic solvents (DESs) and their applications, Chem. Rev. 114 (2014) 11060–11082, <https://doi.org/10.1021/cr300162p>.
- D.T. Wu, K.L. Feng, L. Huang, R.Y. Gan, Y.C. Hu, L. Zou, Deep eutectic solvent-assisted extraction, partially structural characterization, and bioactivities of acidic polysaccharides from lotus leaves, Foods 10 (2021), <https://doi.org/10.3390/foods10102330>.
- J. Xue, J. Su, X. Wang, R. Zhang, X. Li, Y. Li, Y. Ding, X. Chu, Eco-friendly and efficient extraction of polysaccharides from *Acanthopanax senticosus* by ultrasound-assisted deep eutectic solvent, Molecules 29 (2024), <https://doi.org/10.3390/molecules29050942>.
- D. Xu, J. Chow, C.C. Weber, M.A. Packer, S. Baroutian, K. Shahbaz, Evaluation of deep eutectic solvents for the extraction of fucoxanthin from the alga *Tisochrysis lutea* - COSMO-RS screening and experimental validation, J. Environ. Chem. Eng. 10 (2022), <https://doi.org/10.1016/j.jece.2022.108370>.
- N. Ozel, A. Inam, M. Elibol, Exploring deep eutectic solvents for enhanced extraction of bio-active compounds from microalgae biomass, J. Mol. Liq. 407 (2024), <https://doi.org/10.1016/j.molliq.2024.125237>.
- Shang X. Chao, D. Chu, Zhang J. Xu, Zheng Y. Fen, Y. Li, Microwave-assisted extraction, partial purification and biological activity *in vitro* of polysaccharides from bladder-wrack (*Fucus vesiculosus*) by using deep eutectic solvents, Sep. Purif. Technol. 259 (2021), <https://doi.org/10.1016/j.seppur.2020.118169>.

[15] J. Nie, D. Chen, Y. Lu, Deep eutectic solvents based ultrasonic extraction of polysaccharides from edible brown seaweed *Sargassum horneri*, *J. Mar. Sci. Eng.* 8 (2020), <https://doi.org/10.3390/JMSE8060440>.

[16] I.S.A. Hiemstra, J.T. Meinema, M.M.H. Eppink, R.H. Wijffels, A. Kazbar, Choline chloride-based solvents as alternative media for alginate extraction from brown seaweed, *LWT* 214 (2024), <https://doi.org/10.1016/j.lwt.2024.117174>.

[17] L. Yu, Z. Li, W. Huang, A. Ali, Y. Chen, G. Zhao, S. Yao, Recovery and post-treatment processes for ionic liquids and deep eutectic solvents, *J. Mol. Liq.* 402 (2024), <https://doi.org/10.1016/j.molliq.2024.124767>.

[18] M. Sui, S. Feng, J. Yu, B. Chen, Z. Li, P. Shao, Removal and recovery of deep eutectic solvent with membrane-based methodology: a promising strategy to enhance extraction and purification of *Dendrobium officinale* flavonoids, *Ind. Crop. Prod.* 206 (2023), <https://doi.org/10.1016/j.indcrop.2023.117638>.

[19] Y. Wang, F. Xu, J. Cheng, X. Wu, J. Xu, C. Li, W. Li, N. Xie, Y. Wang, L. He, Natural deep eutectic solvent-assisted extraction, structural characterization, and immunomodulatory activity of polysaccharides from *Paecilomyces hepiali*, *Molecules* 27 (2022), <https://doi.org/10.3390/molecules27228020>.

[20] M. Zhang, Z. Zhang, Z. Gu, M. Tian, J. Wang, K. Zheng, C. Zhao, C. Li, Advances of responsive deep eutectic solvents and application in extraction and separation of bioactive compounds, *J. Sep. Sci.* 46 (2023), <https://doi.org/10.1002/jssc.20230098>.

[21] F.A. Vicente, N. Tkalec, B. Likozar, Responsive deep eutectic solvents: mechanisms, applications and their role in sustainable chemistry, *Chem. Commun.* 61 (2024) 1002–1013, <https://doi.org/10.1039/D4CC05157B>.

[22] C. Cai, Y. Wang, W. Yu, C. Wang, F. Li, Z. Tan, Temperature-responsive deep eutectic solvents as green and recyclable media for the efficient extraction of polysaccharides from *Ganoderma lucidum*, *J. Clean. Prod.* 274 (2020), <https://doi.org/10.1016/j.jclepro.2020.123047>.

[23] C. Zhao, Z. Ma, X.X. Zhu, Rational design of thermoresponsive polymers in aqueous solutions: a thermodynamics map, *Prog. Polym. Sci.* 90 (2019) 269–291, <https://doi.org/10.1016/j.progpolymsci.2019.01.001>.

[24] X.Y. Yan, Z.H. Cai, P.Q. Zhao, J.D. Wang, L.N. Fu, Q. Gu, Y.J. Fu, Application of a novel and green temperature-responsive deep eutectic solvent system to simultaneously extract and separate different polar active phytochemicals from *Schisandra chinensis* (Turcz.) Baill, *Food Res. Int.* 165 (2023), <https://doi.org/10.1016/j.foodres.2023.112541>.

[25] Y. Cao, H. Wang, Y. Jian, G. Hao, D. Di, J. Liu, Temperature-switchable deep eutectic solvent extraction of polysaccharides from wolfberry fruits: process optimization, structure characterization, and antioxidant activity, *J. Mol. Liq.* 398 (2024), <https://doi.org/10.1016/j.molliq.2024.124352>.

[26] A. Klamt, Prediction of the mutual solubilities of hydrocarbons and water with COSMO-RS, *Fluid Phase Equilib.* 206 (2003) 223–235, [https://doi.org/10.1016/S0378-3812\(02\)00322-9](https://doi.org/10.1016/S0378-3812(02)00322-9).

[27] D. Xu, J. Chow, C.C. Weber, M.A. Packer, S. Baroutian, K. Shahbaz, Evaluation of deep eutectic solvents for the extraction of fucoxanthin from the alga *Tisochrysis lutea* - COSMO-RS screening and experimental validation, *J. Environ. Chem. Eng.* 10 (2022), <https://doi.org/10.1016/j.jece.2022.108370>.

[28] G.M.C. Silva, D.A. Pantano, S. Loehlé, J.A.P. Coutinho, The challenges of using COSMO-RS to describe polymer solution behavior, *Ind. Eng. Chem. Res.* 62 (2023) 20936–20944, <https://doi.org/10.1021/acs.iecr.3c03310>.

[29] S.Y. Mok, M. Sivapragasam, M.S. Raja Shahrom, M.A. Bustam, Z.Z. Abidin, Screening of ionic liquids for the dissolution of chitosan using COSMO-RS, *Green Chem.* 26 (2023) 1577–1586, <https://doi.org/10.1039/D3gc03586g>.

[30] J. Iqbal, N. Muhammad, A. Rahim, A.S. Khan, Z. Ullah, G. Gonfa, P. Ahmad, COSMO-RS predictions, hydrogen bond basicity values and experimental evaluation of amino acid-based ionic liquids for lignocellulosic biomass dissolution, *J. Mol. Liq.* 273 (2019) 215–221, <https://doi.org/10.1016/j.molliq.2018.10.044>.

[31] D. Wang, M. Zhang, C.L. Law, L. Zhang, Natural deep eutectic solvents for the extraction of lentinan from shiitake mushroom: COSMO-RS screening and ANN-GA optimizing conditions, *Food Chem.* 430 (2024), <https://doi.org/10.1016/j.foodchem.2023.136990>.

[32] B. Ozturk, M. Gonzalez-Miquel, Alkanediol-based deep eutectic solvents for isolation of terpenoids from citrus essential oil: experimental evaluation and COSMO-RS studies, *Sep. Purif. Technol.* 227 (2019), <https://doi.org/10.1016/j.seppur.2019.115707>.

[33] M.A. Al-Maari, H.F. Hizaddin, A. Hayyan, M.K. Hadj-Kali, Screening deep eutectic solvents as green extractants for oil from plant seeds based on COSMO-RS model, *J. Mol. Liq.* 393 (2024), <https://doi.org/10.1016/j.molliq.2023.123520>.

[34] F. Bezold, M.E. Weinberger, M. Minceva, Assessing solute partitioning in deep eutectic solvent-based biphasic systems using the predictive thermodynamic model COSMO-RS, *Fluid Phase Equilib.* 437 (2017) 23–33, <https://doi.org/10.1016/j.fluid.2017.01.001>.

[35] K. Wang, D. Peng, A. Alhadid, M. Minceva, Assessment of COSMO-RS for predicting liquid-liquid equilibrium in systems containing deep eutectic solvents, *Ind. Eng. Chem. Res.* 63 (2024) 11110–11120, <https://doi.org/10.1021/acs.iecr.4c00796>.

[36] M. Cesaretti, E. Luppi, F. Maccari, N. Volpi, A 96-well assay for uronic acid carbazole reaction, *Carbohydr. Polym.* 54 (2003) 59–61, [https://doi.org/10.1016/S0144-8617\(03\)00144-9](https://doi.org/10.1016/S0144-8617(03)00144-9).

[37] N. Gao, Y. Wang, H. Luo, Y. Xu, J. Liu, Y. Chen, pH-switchable hydrophobic deep eutectic solvents for sustainable recycling extraction of high oily waste, *Chem. Eng. J.* 495 (2024), <https://doi.org/10.1016/j.cej.2024.153339>.

[38] X. Chen, R. Wang, Z. Tan, Extraction and purification of grape seed polysaccharides using pH-switchable deep eutectic solvents-based three-phase partitioning, *Food Chem.* 412 (2023), <https://doi.org/10.1016/j.foodchem.2023.135557>.

[39] S. Wang, T. Lei, L. Liu, Z. Tan, CO<sub>2</sub>-responsive deep eutectic solvents for the enhanced extraction of hesperidin from fertile orange peel, *Food Chem.* 432 (2024), <https://doi.org/10.1016/j.foodchem.2023.137255>.

[40] W. Reynaga-Navarro, L. Bozzo, R.H. Wijffels, M. Eppink, A. Kazbar, Characterisation of alginate extracted from *Saccharina latissima* with deep eutectic solvents, *Food Hydrocoll.* 171 (2026), <https://doi.org/10.1016/j.foodhyd.2025.111862>.

[41] H. Bojorges, A. López-Rubio, M.J. Fabra, A. Martínez-Abad, Estimation of alginate purity and M/G ratio by methanolysis coupled with anion exchange chromatography, *Carbohydr. Polym.* 321 (2023), <https://doi.org/10.1016/j.carbpol.2023.121285>.

[42] Shang X. Chao, Zhang Y. Qin, Zheng Y. Fen, Y. Li, Temperature-responsive deep eutectic solvents as eco-friendly and recyclable media for microwave extraction of flavonoid compounds from waste onion (*Allium cepa L.*) skins, *Biomass Convers. Biorefinery* 14 (2024) 3729–3738, <https://doi.org/10.1007/s13399-022-02483-4>.

[43] S.A. Legkov, G.N. Bondarenko, J.V. Kostina, E.G. Novitsky, S.D. Bazhenov, A. V. Volkov, V.V. Volkov, Structural features of Monoethanolamine aqueous solutions with various compositions: a combined experimental and theoretical study using vibrational spectroscopy, *Molecules* 28 (2023), <https://doi.org/10.3390/molecules28010403>.

[44] J.Y. Sung, B.K. Ryu, D.H. Lee, Structure and transmittance behavior of sol-gel silica nanoparticles synthesized using pH-stable alkanolamines, *J. Solgel Sci. Technol.* 85 (2018) 495–503, <https://doi.org/10.1007/s10971-017-4561-2>.

[45] R. Zhang, M. Hong, J. Wu, Y. Xiao, J. Tong, Effect of water on the excess properties of eutectic solvents, *J. Mol. Liq.* 414 (2024), <https://doi.org/10.1016/j.molliq.2024.126139>.

[46] M. López-García, M. Martínez-Cabanas, T. Vilarino, P. Lodeiro, P. Rodríguez-Barro, R. Herrero, J.L. Barriada, New polymeric/inorganic hybrid sorbents based on red mud and nanosized magnetite for large scale applications in as(V) removal, *Chem. Eng. J.* 311 (2017) 117–125, <https://doi.org/10.1016/j.cej.2016.11.081>.

[47] J. Chen, Y. Song, X. Wei, X. Duan, K. Liu, W. Cao, L. Li, G. Ren, Ultrasonic and deep eutectic solvent for efficient extraction of Phenolics from *Eucommia ulmoides* leaves, *Foods* 14 (2025), <https://doi.org/10.3390/foods14060972>.

[48] B. Sun, Y.L. Zheng, S.K. Yang, J.R. Zhang, X.Y. Cheng, R. Ghiladi, Z. Ma, J. Wang, W.W. Deng, One-pot method based on deep eutectic solvent for extraction and conversion of polydatin to resveratrol from *Polygonum cuspidatum*, *Food Chem.* 343 (2021), <https://doi.org/10.1016/j.foodchem.2020.128498>.

[49] M.C. Matchim Kamdem, A.D. Tamafo Fougue, N. Lai, A comprehensive study on DES pretreatment application to microalgae for enhanced lipid recovery suitable for biodiesel production: combined experimental and theoretical investigations, *Energies* 16 (2023), <https://doi.org/10.3390/en16093806>.

[50] M.C. Matchim Kamdem, A.D. Tamafo Fougue, N. Lai, A comprehensive study on DES pretreatment application to microalgae for enhanced lipid recovery suitable for biodiesel production: combined experimental and theoretical investigations, *Energies* (Basel) 16 (2023), <https://doi.org/10.3390/en16093806>.

[51] J. Zhang, S. Li, L. Yao, Y. Yi, L. Shen, Z. Li, H. Qiu, Responsive switchable deep eutectic solvents: a review, *Chin. Chem. Lett.* 34 (2023), <https://doi.org/10.1016/j.ccl.2022.107750>.

[52] W. Zhao, M. Duan, X. Zhang, T. Tan, A mild extraction and separation procedure of polysaccharide, lipid, chlorophyll and protein from *Chlorella spp*, *Renew. Energy* 118 (2018) 701–708, <https://doi.org/10.1016/j.renene.2017.11.046>.

[53] T. Wang, Q. Guo, P. Li, H. Yang, Deep-eutectic solvents/ionic liquids/water mixture as a novel type of green thermo-switchable solvent system for selective extraction and separation of natural products from *Rosmarinus officinalis* leaves, *Food Chem.* 390 (2022), <https://doi.org/10.1016/j.foodchem.2022.133225>.

[54] Z. Tang, Y. Xu, C. Cai, Z. Tan, Extraction of *Lycium barbarum* polysaccharides using temperature-switchable deep eutectic solvents: a sustainable methodology for recycling and reuse of the extractant, *J. Mol. Liq.* 383 (2023), <https://doi.org/10.1016/j.molliq.2023.122063>.

[55] Y. Liu, J. Li, R. Fu, L. Zhang, D. Wang, S. Wang, Enhanced extraction of natural pigments from *Curcuma longa L.* using natural deep eutectic solvents, *Ind. crops, Prod.* 140 (2019), <https://doi.org/10.1016/j.indcrop.2019.111620>.

[56] X. Pan, L. Xu, J. Meng, M. Chang, Y. Cheng, X. Geng, D. Guo, R. Liu, Ultrasound-assisted deep eutectic solvents extraction of polysaccharides from *Morchella importuna*: optimization, physicochemical properties, and bioactivities, *Front. Nutr.* 9 (2022), <https://doi.org/10.3389/fnut.2022.912014>.

[57] X. Chen, R. Wang, Z. Tan, Extraction and purification of grape seed polysaccharides using pH-switchable deep eutectic solvents-based three-phase partitioning, *Food Chem.* 412 (2023), <https://doi.org/10.1016/j.foodchem.2023.135557>.

[58] X. Liang, S. Wang, J. Zhou, T. Lu, K. Ruan, Y. Xia, T. Wang, A novel deep eutectic solvent/switchable-hydrophilicity solvent/H<sub>2</sub>O system with enhanced CO<sub>2</sub> switchability for integrated extraction of phenolics, flavonoids and essential oil from *Flos Chrysanthemi Indici* flower, *Sep. Purif. Technol.* 336 (2024), <https://doi.org/10.1016/j.seppur.2024.126315>.

[59] C. Gao, C. Cai, J. Liu, Y. Wang, Y. Chen, L. Wang, Z. Tan, Extraction and preliminary purification of polysaccharides from *Camellia oleifera* Abel. Seed cake using a thermoseparating aqueous two-phase system based on EOPO copolymer and deep eutectic solvents, *Food Chem.* 313 (2020), <https://doi.org/10.1016/j.foodchem.2020.126164>.

[60] K.I. Draget, C. Taylor, Chemical, physical and biological properties of alginates and their biomedical implications, *Food Hydrocoll.* 25 (2011) 251–256, <https://doi.org/10.1016/j.foodhyd.2009.10.007>.

[61] R. Abka-khajouei, L. Tounsi, N. Shahabi, A.K. Patel, S. Abdelkafi, P. Michaud, Structures, properties and applications of alginates, *Mar. Drugs* 20 (2022), <https://doi.org/10.3390/md20060364>.

[62] G. Mahavishnu, V. Malaiyaran, S.K. Kannaiyan, A. Ramalingam, Investigation of molecular polarity and thermal stability of monoethanolamine based deep eutectic solvents, *J. Dispers. Sci. Technol.* (2024), <https://doi.org/10.1080/01932691.2024.2372691>.

[63] B.S.I. Lasalle, M.S. Pandian, P. Ramasamy, Molecular interactions studies on chloroform in the environment of o-cresol: FTIR spectroscopy and quantum chemical calculations, *Braz. J. Phys.* 53 (2023), <https://doi.org/10.1007/s13538-023-01309-6>.

[64] D. Leal, B. Matsuhiro, M. Rossi, F. Caruso, FT-IR spectra of alginic acid block fractions in three species of brown seaweeds, *Carbohydr. Res.* 343 (2008) 308–316, <https://doi.org/10.1016/j.carres.2007.10.016>.

[65] A. Nesić, M.V. De Bonis, G. Dal Poggetto, G. Ruocco, G. Santagata, Microwave assisted extraction of raw alginates as a sustainable and cost-effective method to Treat Beach-accumulated Sargassum algae, *Polymers (Basel)* 15 (2023), <https://doi.org/10.3390/polym15142979>.

[66] M. Kuzmanović, D.K. Božanić, D. Milivojević, D.M. Ćulafić, S. Stanković, C. Ballesteros, J. González-Benito, Sodium-alginate biopolymer as a template for the synthesis of nontoxic red emitting Mn<sup>2+</sup>-doped CdS nanoparticles, *RSC Adv.* 7 (2017) 53422–53432, <https://doi.org/10.1039/c7ra11011a>.

[67] S.H. Rashedy, M.S.M. Abd El Hafez, M.A. Dar, J. Cotas, L. Pereira, Evaluation and characterization of alginates extracted from brown seaweed collected in the red sea, *Appl. Sci. (Switz.)* 11 (2021), <https://doi.org/10.3390/app11146290>.

[68] W. Jiao, W. Chen, Y. Mei, Y. Yun, B. Wang, Q. Zhong, H. Chen, W. Chen, Effects of molecular weight and Guluronic acid/Mannuronic acid ratio on the rheological behavior and stabilizing property of sodium alginate, *Molecules* 24 (2019), <https://doi.org/10.3390/molecules24234374>.

[69] P.E. Ramos, P. Silva, M.M. Alario, L.M. Pastrana, J.A. Teixeira, M.A. Cerqueira, A. A. Vicente, Effect of alginate molecular weight and M/G ratio in beads properties foreseeing the protection of probiotics, *Food Hydrocoll.* 77 (2018) 8–16, <https://doi.org/10.1016/j.foodhyd.2017.08.031>.

[70] M. Sterner, U. Edlund, Multicomponent fractionation of *Saccharina latissima* brown algae using chelating salt solutions, *J. Appl. Phycol.* 28 (2016) 2561–2574, <https://doi.org/10.1007/s10811-015-0785-0>.

[71] K. Nøkling-Eide, F.L. Aachmann, A. Tøndervik, Ø. Arlov, H. Sletta, In-process epimerisation of alginates from *Saccharina latissima*, *Alaria esculenta* and *Laminaria hyperborea*, *Carbohydr. Polym.* 325 (2024), <https://doi.org/10.1016/j.carbpol.2023.121557>.

[72] I.S.A. Hiemstra, N. Lustig, M.H.M. Eppink, R.H. Wijffels, A. Kazbar, Separation of alginates and recycling of deep eutectic solvents using temperature-responsive aqueous two-phase systems, *J. Clean. Prod.* 536 (2025), <https://doi.org/10.1016/j.jclepro.2025.147186>.

[73] P.S. Saravana, Y.N. Cho, H.C. Woo, B.S. Chun, Green and efficient extraction of polysaccharides from brown seaweed by adding deep eutectic solvent in subcritical water hydrolysis, *J. Clean. Prod.* 198 (2018) 1474–1484, <https://doi.org/10.1016/j.jclepro.2018.07.151>.

[74] M.H. Ng, A.H. Nu'man, A. Hasliyanti, Recycling of deep eutectic solvent in the extraction of ferulic acid from oil palm empty fruit bunch, *J. Sep. Sci.* 47 (2024), <https://doi.org/10.1002/jssc.202300842>.

[75] J. Chen, Y. Xu, Z. Tan, CO<sub>2</sub>-triggered switchable hydrophilicity solvent as a recyclable extractant for ultrasonic-assisted extraction of *Polygonatum sibiricum* polysaccharides, *Food Chem.* 402 (2023), <https://doi.org/10.1016/j.foodchem.2022.134301>.

[76] N. Gao, Y. Wang, H. Luo, Y. Xu, J. Liu, Y. Chen, pH-switchable hydrophobic deep eutectic solvents for sustainable recycling extraction of high oily waste, *Chem. Eng. J.* 495 (2024), <https://doi.org/10.1016/j.cej.2024.153339>.

[77] X. Zhang, X. Yan, Z. Cai, L. Fu, X. Dong, J. Cui, H. Zheng, M. Xu, Y. Fu, A novel and green temperature-responsive biphasic deep eutectic solvent-based system for simultaneous extraction and pre-separation of active ingredients from *Zanthoxylum bungeanum maxim.* Peels. Ind crops, *Prod* 221 (2024), <https://doi.org/10.1016/j.indrop.2024.119324>.

[78] L.T. Wu, Y.T. Zhan, Z.L. Li, P.T. Chen, B.J. Hwang, J.C. Jiang, Rational electrolyte design for Li-metal batteries operated under extreme conditions: a combined DFT, COSMO-RS, and machine learning study, *J Mater Chem A Mater* 12 (2024) 15792–15802, <https://doi.org/10.1039/d4ta03026e>.